Dynamics of anomalous optical transitions in $Al_xGa_{1-x}N$ alloys

Yong-Hoon Cho,* G. H. Gainer, J. B. Lam, and J. J. Song
Center for Laser and Photonics Research and Department of Physics, Oklahoma State University, Stillwater, Oklahoma 74078

W. Yang
Honeywell Technology Center, 12001 State Highway 55, Plymouth, Minnesota 55441

W. Jhe
Center for Near-field Atom-photon Technology and Department of Physics, Seoul National University, Seoul 151-742, Korea
(Received 17 May 1999)

We present a comprehensive study of the optical characteristics of $Al_xGa_{1-x}N$ epilayers ($0 \leqslant x \leqslant 0.6$) by means of photoluminescence (PL), PL excitation, and time-resolved PL spectroscopy. For $Al_xGa_{1-x}N$ with large Al content, we observed an anomalous PL temperature dependence: (i) an ''S-shaped'' PL peak energy shift (decrease-increase-decrease) and (ii) an ''inverted S-shaped'' spectral width broadening (increase-decrease-increase) with increasing temperature. We observed that the thermal decrease in integrated PL intensity was suppressed and the effective lifetime was enhanced in the temperature region showing the anomalous temperature-induced emission behavior, reflecting superior luminescence efficiency by suppressing nonradiative processes. All these features were enhanced as the Al mole fraction was increased. From these results, the anomalous temperature-induced emission shift is attributed to energy tail states due to alloy potential inhomogeneities in the $Al_xGa_{1-x}N$ epilayers with large Al content.

Much interest has been focused on (Al, In)GaN alloys and their heterostructures, whose band gap energy varies between 6.2 and 1.9 eV at room temperature, due to their potential applications such as red-ultraviolet (UV) light emitting devices,[1,2] solar-blind UV detectors,[3] and high-power and high-temperature devices.[4,5] In particular, the ternary compound $Al_xGa_{1-x}N$ has the potential for use in light-emitting and light-detecting devices covering nearly the entire deep-UV region of the spectrum (3.4–6.2 eV). In spite of poor structural properties (e.g., high threading dislocation density $>10^{10}$ cm^{-2}) due to large lattice and thermal mismatches, it has been demonstrated that InGaN-based light-emitting devices are highly efficient and have very low thresholds, and it is believed that the recent success of achieving InGaN-based light-emitting devices is deeply related to the role of carriers localized in the InGaN active region. In the InGaN-based light-emitting device structures, In alloy inhomogeneity and/or quantum-dot-like In phase separation have been proposed as the cause of the localized states,[6–10] and an anomalous temperature dependence of the InGaN emission peak energy due to band-tail states was observed.[11–13] According to thermodynamical calculations, however, ternary AlGaN alloys are predicted to not have an unstable mixing region, in contrast to InGaN and InAlN alloys. Therefore, no phase separation is expected in AlGaN alloys.[14] Although understanding the emission mechanism and the role of the energy tail states in (Al, In)GaN alloys is very important, the detailed emission properties of AlGaN-based structures have not previously been clarified, in contrast to the case of InGaN-based structures.

In this paper, we report optical properties of $Al_xGa_{1-x}N$ epilayers ($0 \leqslant x \leqslant 0.6$) as a function of temperature using photoluminescence (PL), PL excitation (PLE), and time-resolved PL (TRPL) spectroscopy. By studying alloy epilayers instead of quantum structures, one can avoid ambiguous effects usually involved in quantum structures, such as strain-induced piezoelectric polarization, quantum confinement, layer thickness variations, and interface-related defects. The $Al_xGa_{1-x}N$ thin films used in this work were grown by metalorganic chemical vapor deposition (MOCVD) on (0001)-oriented sapphire. A set of samples, nominally identical aside from deliberate variations in the Al content x of the $Al_xGa_{1-x}N$ alloys, were grown specifically to study the influence of x in the $Al_xGa_{1-x}N$ alloys. The growth temperature was about 1050 °C. Prior to $Al_xGa_{1-x}N$ growth, a thin ~5-nm-thick AlN buffer layer was deposited on the sapphire at a temperature of 625 °C. Triethylgallium, triethylaluminum, and ammonia were used as precursors in the $Al_xGa_{1-x}N$ growth. The $Al_xGa_{1-x}N$ layer thickness was about 1 μm. To evaluate the Al alloy composition and to check for ordering effects, the samples were analyzed with high-resolution x-ray diffraction (XRD) measurements using Cu $K\alpha_1$ radiation. PL and PLE experiments were performed using the 244-nm line of an intracavity doubled cw Ar^+ laser and quasimonochromatic light emission from a Xe lamp dispersed by a 1/2-m monochromator as an excitation source, respectively. TRPL measurements were carried out using a picosecond pulsed laser system consisting of a cavity-dumped dye laser synchronously pumped by a frequency-doubled mode-locked Nd:YAG (yttrium aluminum garnet) laser for sample excitation and a streak camera for detection.

Figure 1 shows 10-K PL and PLE spectra for $Al_xGa_{1-x}N$ epilayers with $x=0.17$, 0.26, 0.33, and 0.6 with a PL peak energy (E_{PL}) of ~3.70, 3.92, 4.22, and 4.76 eV, respectively. The PL spectra were measured using second-order diffraction through a monochromator and all the spectra were normalized. The decrease in PLE signal above the PLE

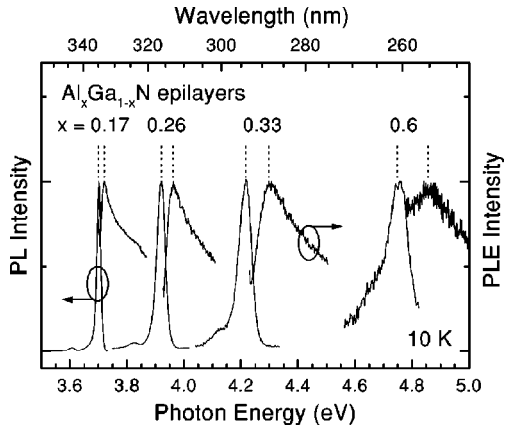

FIG. 1. 10-K PL and PLE spectra of $Al_xGa_{1-x}N$ epilayers with Al content $x = 0.17$, 0.26, 0.33, and 0.60. A Stokes shift of the PL emission from the $Al_xGa_{1-x}N$ with respect to the band edge measured by PLE increases with increasing x.

peak position with increasing excitation energy is due to the decrease in the excitation intensity of a Xe lamp source. Note that the full width at half maximum (FWHM) of the PL emission and the Stokes shift between the PL emission peak energy and the PLE absorption edge monotonically increase with varying x from 0 to 0.6.

Figure 2 shows the evolution of PL spectra as a function of temperature for the $Al_xGa_{1-x}N$ epilayers with $x=0.17$, 0.26, and 0.33. In general, the emission peak energy follows the well-known temperature dependence of the energy gap shrinkage, $E_g(T)=E_g(0)-\alpha T^2/(\beta+T)$, where $E_g(T)$ is the band-gap transition energy at a temperature T, and α and β are known as the Varshni thermal coefficients.[15] The parameters $\alpha=8.32\times10^{-4}$ eV/K and $\beta=835.6$ K for the GaN Γ_9^v-Γ_7^c transition were previously extracted by photoreflectance studies.[16] The temperature-dependent PL peak shift for the GaN and $Al_xGa_{1-x}N$ layers with small x value ($x<0.1$) was consistent with the estimated energy decrease. On

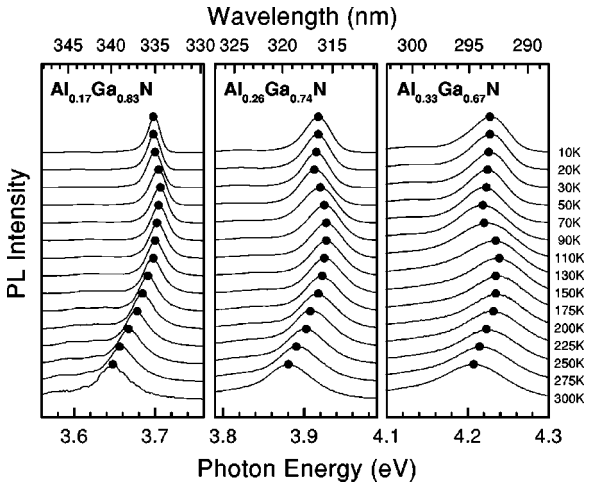

FIG. 2. PL spectra for $Al_xGa_{1-x}N$ epilayers in the temperature range from 10 to 300 K. The emission peak shows an anomalous S-shaped shift behavior with increasing temperature (solid circles). Note that the crossover temperature from redshift to blueshift increases with increasing x. All spectra are normalized and shifted in the vertical direction for clarity.

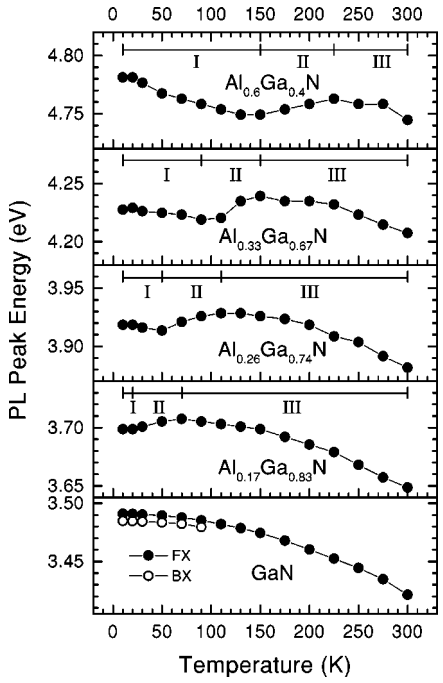

FIG. 3. PL peak energies for $Al_xGa_{1-x}N$ epilayers in the temperature range from 10 to 300 K. The emission peak shows an anomalous S-shaped shift behavior with increasing temperature. The temperature regions I, II, and III correspond to redshift, blueshift, and redshift behavior of the PL peak positions. The free exciton (FX) and bound exciton (BX) curves are shown for GaN.

the other hand, the PL emission from $Al_xGa_{1-x}N$ with higher x did not follow the typical temperature dependence of the energy gap shrinkage and has interesting attributes not seen in random homogeneous III-V alloys. E_{PL} clearly shows the ''S-shaped'' emission shift (decrease-increase-decrease) behavior with increasing temperature. For the $Al_xGa_{1-x}N$ epilayer with $x=0.17$ (0.26, 0.33, 0.6), with increasing temperature up to T_I, where T_I is $\sim$20 (50, 90, 150) K, an initial small decrease in E_{PL} was observed, followed by an increase in E_{PL} in the temperature range of T_I-T_{II}, where T_{II} is $\sim$70 (110, 150, 225) K, and finally E_{PL} decreased again as the temperature increased above T_{II}. Another unusual property of the PL spectra is that the FWHM shows an anomalous ''inverted S-shaped'' FWHM broadening (increase-decrease-increase) behavior with increasing temperature. The PL peak energy position of the $Al_xGa_{1-x}N$ epilayers with $x=0$, 0.17, 0.26, 0.33, and 0.6 are plotted as a function of temperature in Fig. 3. The temperature-induced ''initial'' redshift (region I), blueshift (region II), and ''final'' redshift (region III) behavior of the PL peak position are clearly shown for $x=0.17$, 0.26, 0.33, and 0.6, in contrast to the case of $x=0$ (GaN). Note that the corresponding temperature regions significantly depend on x: with increasing x, the characteristic temperatures T_I and T_{II} increase and the temperature regions I and II are extended into higher temperatures.

One would suspect that the energy difference (ΔE) between the PL peak at $T<T_I$ and the $E_g(T<T_I)$ determined by $E_g(T)=E_g(0)-\alpha T^2/(\beta+T)$ using the measured peak energies at $T>T_{II}$ would correspond to the binding energy of excitons bound at neutral donors (or acceptors). In the case of GaN, ΔE between the bound exciton (BX) and the free

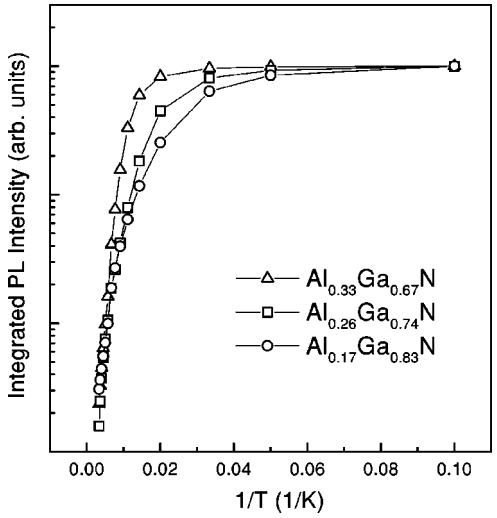

FIG. 4. Normalized integrated PL intensity as a function of temperature for the $Al_xGa_{1-x}N$-related emission of $Al_xGa_{1-x}N$ epilayers with Al content $x=0$, 0.17, 0.26, and 0.33. Activation energies estimated from the relationship $I_{PL}=I_0/[1+A\exp(-E_a/kT)]$ in the transition region II are 9.6 ± 1.5, 21.2 ± 1.2, and 44.6 ± 1.8 meV for the $Al_xGa_{1-x}N$ epilayers with $x=0.17$, 0.26, and 0.33, respectively, indicating more confinement with increasing x.

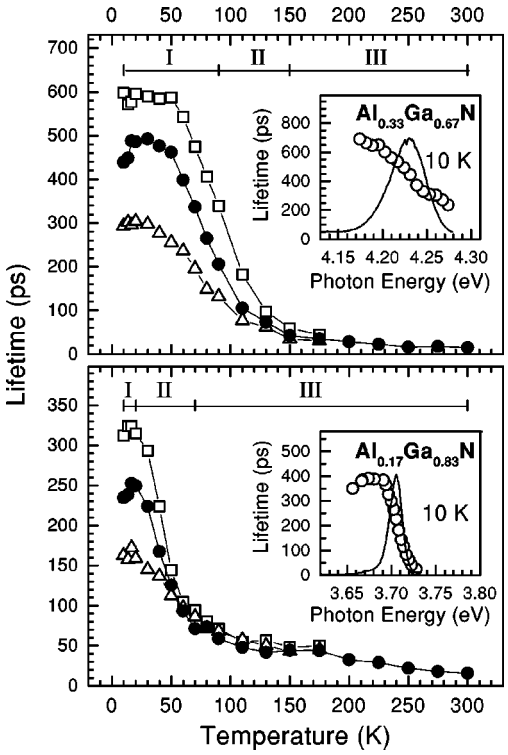

FIG. 5. Lifetime as a function of temperature for the emission in $Al_xGa_{1-x}N$ epilayers with $x=0.17$ and 0.33. The insets show the emission energy dependence of lifetime. Note that the lower-energy side of the PL peak has a longer lifetime than the higher-energy side for $T<T_{II}$, while there is no difference between lifetimes monitored above (open triangles), below (open squares), and at (closed circles) the peak energy for $T>T_{II}$.

exciton (FX) energies is about 6 meV, which corresponds exactly to the BX-to-FX transition temperature $\Delta E/k$ of $\sim$70 K. In contrast, for the $Al_xGa_{1-x}N$ epilayer with $x=0.17$ (0.26, 0.33, 0.6), $\Delta E/k$ is much larger than the characteristic transition temperature $T_{II}\sim70$ (110, 150, 225) K (see Fig. 3). Therefore, the temperature-induced optical transitions in the $Al_xGa_{1-x}N$ epilayers are not due to the BX-to-FX transition as seen in the GaN layers. In addition, we observed no PL peak energy shift by varying excitation density over four orders of magnitude for all the samples, indicating that the transition is not due to donor-acceptor pair related recombination, since the Coulomb interaction of donors and acceptors as a function of their separation would lead to a shift in emission energy with excitation density. On the other hand, a similar anomalous temperature dependence for PL peak energy has been reported in ordered $GaInP_2$ (i.e., a monolayer superlattice of GaP and InP formed on the group-III sublattice) and in disordered superlattices consisting of $(AlAs)_m(GaAs)_n$ with m and n randomly chosen, in contrast to the case of random homogeneous direct gap III-V alloys (e.g., $Al_xGa_{1-x}As$, disordered $GaInP_2$, etc.) or ordered AlAs/GaAs superlattices (e.g., periods of two monolayers of AlAs and two monolayers of GaAs). Recently, there have been some reports on the long-range ordering effect in molecular beam epitaxy-grown InGaN and AlGaN films.[17] To determine if ordered domains are in our $Al_xGa_{1-x}N$ alloys, XRD measurements were made. However, no (0001) XRD patterns were observed, indicating an absence of the ordered domains in the $Al_xGa_{1-x}N$ alloys under investigation. Therefore, we rule out the possibility of the ordering effect in the $Al_xGa_{1-x}N$ alloys. The AlGaN alloys clearly show interesting emission behavior which cannot be explained in terms of conventional *homogeneous* alloy fluctuations or an ordering effect. In addition, thermodynamic theory predicts that there is no phase separation in the AlGaN alloys.[14]

To investigate the temperature dependence of the quantum efficiency η and the carrier dynamics of the transition from the lower ''localized'' states in the alloys, we carried out integrated PL intensity and TRPL measurements, respectively, over the same temperature range. Figure 4 shows Arrhenius plots of the normalized integrated PL intensities (I_{PL}) over the temperature range of 10–300 K. The main difference between the I_{PL} curves occurs in the temperature range showing the abnormal temperature dependence (i.e., regions I and II). An activation energy (E_a) estimated from the relationship $I_{PL}=I_0/[1+A\exp(-E_a/kT)]$ in the transition region II corresponds to the magnitude of effective potential fluctuations. The activation energies are 9.6 ± 1.5, 21.2 ± 1.2, and 44.6 ± 1.8 meV for the $Al_xGa_{1-x}N$ epilayers with $x=0.17$, 0.26, and 0.33, respectively, reflecting more effective confinement with increasing x. We note that the increase in the thermal activation energy with increasing Al content is in good agreement with the increase in the Stokes shift between the PL peak energy and the PLE absorption edge (see Fig. 1). These E_a values are also well matched with the ΔE values obtained from Fig. 3. Figure 5 shows the temperature dependence of the TRPL lifetimes, and the insets show the 10-K lifetimes as a function of emission energy (open circles) with time-integrated PL spectra for the $Al_{0.17}Ga_{0.83}N$ and $Al_{0.33}Ga_{0.67}N$ thin films. The lifetimes τ_d were monitored at the peak energy (closed circles), lower-energy side (open squares) and higher-energy side (open triangles) of the peak position for the $Al_{0.17}Ga_{0.83}N$ and $Al_{0.33}Ga_{0.67}N$ epilayers. We observed that the FWHM is

about 17 and 48 meV and the overall lifetime is about 250 and 450 ps at 10 K for the $Al_{0.17}Ga_{0.83}N$ and $Al_{0.33}Ga_{0.67}N$ thin films, respectively. In both cases, the measured lifetime increases with decreasing emission energy, and hence, the peak energy of the emission shifts to the low energy side as time proceeds. This characteristic feature can be attributed to inhomogeneous potential fluctuations in the $Al_xGa_{1-x}N$ alloys.[11]

Although the lifetimes as a function of temperature are different for the two samples, one can find interesting common features of the samples from this analysis, as follows. In temperature region I, the change in the measured lifetime is very small and the difference between the lifetimes measured above, below, and at the peak energy is quite large, indicating that radiative recombination processes are dominant. As the temperature is further increased, the overall lifetime quickly decreases in region II and is almost constant in region III, reflecting a strong influence of nonradiative recombination processes. This is further evidenced by a quick decrease in the difference between lifetimes measured above, below, and at the peak energy in region II and no difference through region III. Assuming η of 100% at $T=10$ K and using the equation of $I_{\mathrm{PL}}(T)/I_{\mathrm{PL}}(10\ \mathrm{K}) \approx \eta(T) = \tau_{tot}(T)/\tau_r(T)$, one can determine the radiative and nonradiative lifetimes as a function of temperature. The total lifetime τ_{tot} is given by $1/\tau_{tot}=1/\tau_r+1/\tau_{nr}$, where τ_r is the radiative lifetime and τ_{nr} is the nonradiative one. Using the relationship between $\eta(T)$ and $\tau(T)$, we found that the transition from radiative to nonradiative recombination occurs at ~ 30 and ~ 80 K for the $Al_{0.17}Ga_{0.83}N$ and $Al_{0.33}Ga_{0.67}N$ thin films, respectively. Consequently, radiative recombination is dominant for $T<T_I$ (region I), and the transition from radiative to nonradiative recombination occurs at about T_I, for both samples. In region II, in which a blueshift of the PL peak energy was observed, nonradiative recombination becomes dominant, so the lifetimes and their differences dramatically decrease. In region III, a typical temperature dependence of PL spectra was observed and no sudden change of lifetime occurs.

From the TRPL results, together with the S shape (inverted S shape) of the PL peak position (FWHM) as a function of temperature and the much smaller PL intensity decrease in the temperature range showing the anomalous emission behavior, we conclude that strong localization of carriers occurs in $Al_xGa_{1-x}N$ with rather high Al content. This is quite surprising since the $Al_xGa_{1-x}N$ ternary alloys investigated have neither ordering effects nor phase separations (according to theoretical prediction[14]), and most *homogeneous* ternary alloys do not show such an anomalous emission behavior. Finally, it should be noted that (i) the Stokes-like shift, (ii) the deviations of the PL peak energy, FWHM, and PL intensity from their typical temperature dependence, and (iii) the corresponding temperature ranges (regions I and II) increase with increasing x of the $Al_xGa_{1-x}N$ epilayers. Therefore, we conclude that the anomalous emission is due to optical transitions from ''localized'' to ''extended'' band-tail states, and the band-gap fluctuation responsible for the deviations enhanced with increasing x can be attributed to energy tail states due to *inhomogeneous* alloy potential fluctuations *nonrandomly distributed* in the plane of the layers.[18] Detailed studies are under way to clarify the origins which cause deviations from randomness in the $Al_xGa_{1-x}N$ alloys.

In summary, we have investigated the optical characteristics of MOCVD-grown $Al_xGa_{1-x}N$ ($0 \leqslant x \leqslant 0.6$) epilayers by means of PL, PLE, and TRPL spectroscopy. We observed anomalous temperature-induced PL emission behavior for $Al_xGa_{1-x}N$ epilayers: an ''S-shaped'' PL peak energy shift (decrease-increase-decrease) and an ''inverted S-shaped'' PL FWHM broadening (increase-decrease-increase) with increasing temperature. The deviation from the typical temperature dependence of PL spectra and the temperature range in which the anomalous emission behavior occurs increase with increasing Al content of the $Al_xGa_{1-x}N$ epilayers. From the integrated PL intensity and lifetime measurements as a function of temperature, we found that the anomalous temperature-induced emission shift is deeply related to thermal population in localized energy tail states due to alloy potential inhomogeneities in the $Al_xGa_{1-x}N$ epilayers. Therefore, we attribute the anomalous emission behavior to the enhanced band-gap fluctuation in $Al_xGa_{1-x}N$ epilayers caused by an inhomogeneous spatial distribution of the Al content, and the degree of band-gap fluctuation increases with increasing x.

The authors would like to acknowledge the contributions of Dr. Y. H. Kwon for the XRD measurements. This work was supported by AFOSR, ARO, ONR, DARPA, and CRI of MOST.

*Present address: Center for Near-field Atom-photon Technology and Department of Physics, Seoul National University, Seoul 151-742, Korea. Electronic address: lionsun@phya.snu.ac.kr

[1] S. Nakamura *et al.*, Jpn. J. Appl. Phys., Part 2 **34**, L1332 (1995).
[2] S. Nakamura *et al.*, Appl. Phys. Lett. **69**, 4056 (1996).
[3] B. W. Lim *et al.*, Appl. Phys. Lett. **68**, 3761 (1996).
[4] Y. F. Wu *et al.*, Appl. Phys. Lett. **69**, 1438 (1996).
[5] X. H. Yang *et al.*, Appl. Phys. Lett. **66**, 1 (1995).
[6] S. Chichibu *et al.*, Appl. Phys. Lett. **69**, 4188 (1996).
[7] E. S. Jeon *et al.*, Appl. Phys. Lett. **69**, 4194 (1996).
[8] P. Perlin *et al.*, Appl. Phys. Lett. **70**, 2993 (1997).
[9] Y. Narukawa *et al.*, Appl. Phys. Lett. **70**, 981 (1997).
[10] Y. Narukawa *et al.*, Phys. Rev. B **55**, R1938 (1997).
[11] Y. H. Cho *et al.*, Appl. Phys. Lett. **73**, 1370 (1998).
[12] P. G. Eliseev *et al.*, Appl. Phys. Lett. **71**, 569 (1997).
[13] K. G. Zolina *et al.*, MRS Internet J. Nitride Semicond. Res. **1**, 11 (1996).
[14] T. Matsuoka, MRS Internet J. Nitride Semicond. Res. **3**, 54 (1998).
[15] Y. P. Varshni, Physica (Amsterdam) **34**, 149 (1967).
[16] W. Shan *et al.*, Appl. Phys. Lett. **66**, 985 (1995).
[17] D. Korakakis *et al.*, Appl. Phys. Lett. **71**, 72 (1997).
[18] For the $Al_{0.6}Ga_{0.4}N$ sample, strictly speaking, the inhomogeneous spatial distribution of Ga atoms causes the band-gap potential fluctuations, since Ga atoms replace Al sites in $Al_xGa_{1-x}N$ alloys with $x>0.5$.